Investigation of Carbon near the Graphite-Diamond-Liquid Triple Point

S. Prawer and D. N. Jamieson
School of Physics, University of Melbourne, Parkville, Victoria, 3052, Australia

R. Kalish
Department of Physics and Solid State Institute, Technion, Haifa, Israel
(Received 17 April 1992)

Pulsed laser irradiation is used to heat deeply buried damage layers in diamond. Over a small range of laser powers, annealing of damage, formation of buried graphitic layers, and melting of diamond followed by its conversion upon cooling into graphite are observed. The diagnostics employed are channeling contrast microscopy, optical absorption, surface profilometry, and scanning and optical microscopies. The results are explained in terms of the behavior of carbon under high internal pressures close to the diamond-graphite-liquid triple point in the phase diagram.

PACS numbers: 81.30.Dz, 61.70.At, 61.80.Jh, 64.70.Dv

Fascination with carbon stems from its ability to form very different types of solids, ranging from soft, electrically conducting graphite to hard, electrically insulating diamond, with many intermediate noncrystalline forms in between. The phase diagram of carbon (see Fig. 1 [1]) shows, in addition to graphite and diamond, the existence of a liquid phase of carbon. The different zones in the phase diagram of carbon have been studied both experimentally [1] and theoretically [2]. However, none of the experimental studies have probed the regime around the triple point connecting the diamond-graphite-liquid zones in the phase diagram (see Fig. 1).

In the present Letter we report on results which address this important, yet unexplored zone in the carbon phase diagram. Use is made of high internal pressure which prevails inside a buried damage layer in diamond created by deep ion implantation and of its local heating by selective absorption of intense, sharply convergent, short laser pulses. The laser-treated spots show, over a narrow range of increasing laser power, not only diamond regrowth, but also internal graphitization and sudden loss of the entire undamaged diamond cap layer (1.5 μm thick).

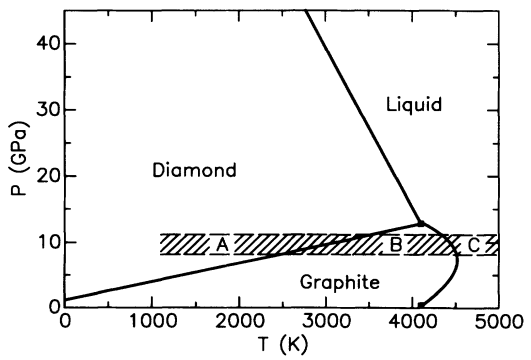

FIG. 1. The phase diagram of carbon (after Bundy [1]). The hatched area designates the region explored in the present work as explained in the text.

The samples used were optically polished, ⟨110⟩-oriented, type-IIa diamond slabs ($3\times3\times0.25$ mm^3). A deeply buried layer of damage was produced by implantation with 2.8-MeV C^+ ions ($R_p \pm \Delta R_p = 1.48 \pm 0.06$ μm), leaving an almost undamaged surface cap of diamond about 1 μm thick [3]. In order to avoid the formation of more complex defect structures, the implantation was carried out at 77 K, a temperature at which both interstitials and vacancies are believed to be immobile [4]. For room-temperature 90-keV implants above a dose of 2.5×10^{15} C^+/cm^2, radiation-damaged diamond converts to graphite upon furnace annealing [5]. Hence, the doses employed here were (1, 2, and 3)$\times10^{15}$ C^+/cm^2. The laser used was a passively Q-switched, frequency-doubled (531 nm), Nd-silicate-glass laser, which was focused through a conventional $\times4$ objective lens onto the sample in air. The pulse width was 14 ns with a spot size of approximately 10 μm. At a wavelength of 531 nm the laser light is selectively absorbed by the damaged region which has an absorption coefficient estimated from optical absorption on the 3×10^{15} C^+/cm^2 specimen to be about 2×10^4 cm^{-1}. By contrast, undamaged diamond is transparent at this wavelength. Thus energy is selectively deposited into the damaged layer, which is sandwiched from both sides by nearly undamaged diamond, producing, in effect, a microscopic high-pressure cell for the radiation-damaged layer. It is important to note that in the absence of an undamaged surface cap, absorption of high-power (up to 60 J/cm^{2}pulse) laser irradiation ablates or graphitizes diamond [6]. Previous work by Sandhu *et al.* [7] also showed that a constraining cap layer can be used to inhibit graphitization during rapid thermal and furnace annealing. However, laser annealing differs from furnace and rapid thermal annealing in that much higher temperatures are obtainable, selective heating of the buried layer is possible by careful choice of the irradiation wavelength, spatial selectivity is achievable, and different annealing mechanisms probably operate due to the very short anneal times (ns).

The pressure extant inside the buried layer was measured using confocal Raman microscopy. For a sample irradiated with 2×10^{15} C^+/cm^2, the Raman spectrum returned from the cap layer showed a downward Raman shift of 7.7 cm^{-1} as compared to the peak position returned from the undamaged diamond substrate. Using the uniaxial-stress dependence of the Raman phonon frequency [8] this shift corresponds to an internal stress of between 4 and 5 GPa. An alternative estimate of the stress P can be obtained via $P=Y(\Delta x/x)$, where Y is Young's modulus (1055 GPa for diamond), Δx is the implantation-induced swelling, and x is the thickness of the cap. For the observed swelling of 100 nm for a dose of 2×10^{15} C^+/cm^2, the calculated pressure is 7 GPa, in approximate agreement with the result from Raman scattering. For a higher dose of 3×10^{15} C^+/cm^2, the swelling is 200 nm, giving an estimate of the pressure inside the buried layer of 8–10 GPa.

The properties characteristic of ion-implantation damage in diamond include (i) the introduction of optical absorption in the visible, in particular the appearance of the GR-1 absorption band [9]; (ii) the disruption of the diamond crystallinity, as observed by ion-channeling experiments; (iii) the swelling of the implanted diamond due to the creation of immobile (at an irradiation temperature of 77 K) vacancies and interstitials, and (iv) the disappearance of the extreme resistance of diamond to etching by concentrated, boiling acids which is typical for diamond, but not for graphite.

The efficacy of laser annealing of the radiation damage has been assessed by monitoring the laser-induced variation of the above properties. Optical microscopy and optical transmission measurements (400–800 nm) have been used to monitor the bleaching of the ion-implantation-induced darkening. The amount of regrowth has been assessed using channeling contrast microscopy (CCM) [10]. This technique employs a focused beam of MeV ions which is scanned over the region of interest on the specimen which has been aligned in a channeling orientation with respect to the probing ion beam. The backscattered yield is recorded as a function of position on the sample, enabling an image to be generated in which the contrast is due to differences in crystalline quality between different regions of the specimen. It is then possible to extract from any region of the image the channeled backscattering spectrum. The present work employed a beam of 1.4-MeV H^+ ions focused down to a 1.5-μm-diam spot. A surface profilometer was used to monitor swelling of the implanted portions of the sample, compaction accompanying annealing, and material loss due to ablation and graphitization. Complete graphitization through to the surface was assumed to have occurred for those laser-treated spots which initially appeared black, but turned transparent following chemical etching in boiling acids known to attack graphite but not diamond [11].

Figure 2 shows optical micrographs and CCM images of the changes which take place following irradiation with ever increasing laser power densities. The absolute values of power density I delivered to the specimen are subject to errors of up to 50% due to uncertainties in the determination of the spatial pulse profile. However, the relative values are reliable to within the pulse-to-pulse power variation of the laser which was measured to be less than 5%. At the lowest powers ($I<10$ J/cm^{2}pulse) no visible effect is observed, with the implanted diamonds retaining their ion-beam-induced brownish color. As the power is increased into the range $10<I<23$ J/cm^{2}pulse very marked bleaching of this color is observed [Fig. 2(a)]; however, the transparency of the laser-irradiated spot does not reach that of the unimplanted diamond. At yet

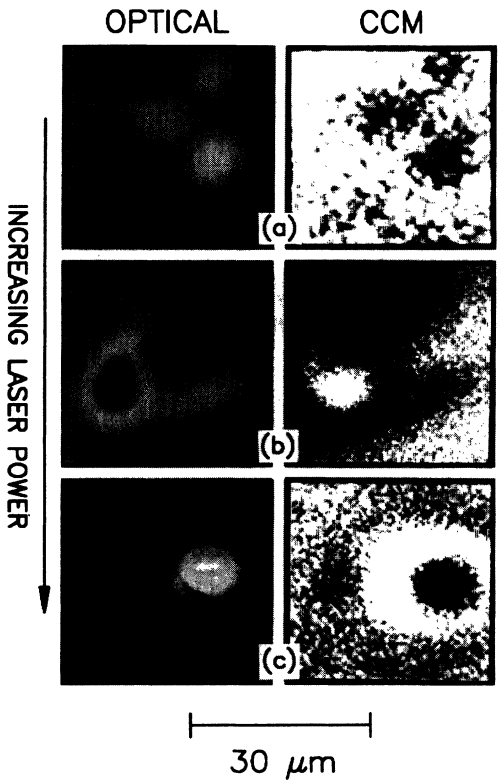

FIG. 2. Transmitted white light optical images and channeling contrast microscopy (CCM) images of laser-irradiated, radiation-damaged (3×10^{15} C^+/cm^2 at 2.8 MeV) diamond. In the optical images, damaged diamond appears dark and annealed or undamaged diamond appears light. In the corresponding CCM images, annealed diamond, which produces a low-intensity backscattered yield, appears dark. Top row (a): Three low-power ($I<23$ J/cm^{2}pulse) laser spots which have caused partial regrowth. Middle row (b): Intermediate laser powers ($23<I<28$ J/cm^{2}pulse) produce a buried brown spot which has a high backscattered yield but is surrounded by a halo of annealed material. Bottom row (c): High laser power ($I>30$ J/cm^{2}pulse) causes graphitization of the entire surface cap which after chemical etching reveals the underlying high-quality crystal. Swelling of the surrounding material producing a halo of misaligned crystal appears as a bright annulus in the CCM image.

higher powers ($23 < I < 28$ J/cm^{2}pulse) a dark brown or indeed in some cases even a pitch black spot is observed in the center of the bleached region [Fig. 2(b)]. These dark spots are found to be totally resistant to etching by the hot acids, showing that an intact diamond surface cap is still present and that these darker regions are deeply buried, a conclusion also supported by their channeling spectra (see below). At yet higher powers ($I > 30$ J/cm^{2}pulse) the entire spot turns black, but, in contrast with the dark spots shown in Fig. 2(b), all the graphite is removed following acid etching leaving a transparent region behind [Fig. 2(c)]. Step height measurements, scanning electron microscopy, and channeling spectra (see below) confirmed that the full cap layer (1.5 μm thick) is removed by this combination of high-power laser irradiation and subsequent acid etching. It is important to note that no intermediate amounts of material loss which could be attributed to simple ablation [6] are observed in any of the dozens of laser spots investigated. Any graphitization observed on the surface is always accompanied by the transformation of the entire surface cap including the buried damage layer.

The CCM images in Fig. 2 have been produced so that darker regions correspond to areas on the sample which return a lower backscattered yield (i.e., better-quality crystal). In Fig. 3, channeling backscattering spectra are shown which have been extracted from the subregions of interest previously discussed. Figure 3 shows a typical spectrum from an annealed spot (curve *a*) which shows considerable regrowth of the damaged region (χ_{min} $=3.3\%$ at 1000 keV) when compared to the spectrum from the as-implanted region. Also shown is the spectrum extracted from a brown spot within an annealed spot (*b*), which shows significant dechanneling characteristic of graphitic material. Spectra extracted from the halo region surrounding the brown spots (not shown) were similar to those obtained from the annealed spot (*a*). Finally, the spectrum from the crater left following complete graphitization and acid treatment is shown in Fig. 3, curve *c*. This spectrum is almost identical to that from an unimplanted diamond apart from a substantial surface peak.

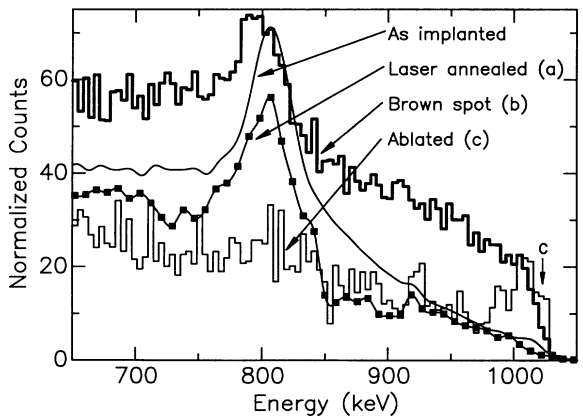

FIG. 3. Channeling backscattering spectra from the regions of interest from the images in Fig. 2. The low-power laser spots (curve *a*) show significant regrowth of the surface and buried damage layers, whereas the spectrum from the buried graphite spot (curve *b*) shows significant dechanneling almost through to the surface indicating a thick, buried, graphitic layer. The center of the ablated region (curve *c*) shows mainly virgin diamond, but with a thin damaged layer at the bottom of the crater. Also shown for comparison is the spectrum from the as-implanted region of the diamond revealing a damage peak due to the end of range damage at a depth of 1.5 μm below the surface.

All the data shown in Figs. 2 and 3 are for a diamond initially irradiated with 3×10^{15} C$^+$/cm^2. Similar results were obtained for the lower-dose specimens, except that the phenomenon of the black spot in the center of the bleached region was not observed and the annealing was more complete [12]. By using multiple pulses of progressively higher power, almost complete annealing is possible [13].

Optical absorption measurements on the laser-annealed spots complement the above results. In the region of the *GR*-1 band at 550 nm the optical transmission of samples normalized to unimplanted diamond were measured to be 44%, 38%, and 31% for doses of (1, 2, and 3)$\times10^{15}$ C$^+$/cm^2, respectively. Following successful laser annealing the transmission increased to 90%, 85%, and 70%, respectively, showing that the laser treatment has been effective in reducing the number of optically active defects.

Step height measurements across the boundary between an unimplanted and an implanted region yield a swelling of 20 nm for a dose of 3×10^{15} C$^+$/cm^2. This swelling is attributable to the buildup of vacancies in the ion-implanted layer [14]. Step height measurements across bleached spots revealed a compaction of about 5 nm. This value is consistent with all the above observations showing considerable laser annealing of the ion-beam-induced damage. By contrast, surface profilometry of fully graphitized and etched regions [Fig. 2(c)] showed the presence of deep craters at least 1 μm deep with very sharp walls, owing to the complete removal of the surface cap and the buried damaged layer.

From the above results, three distinct responses of the damaged diamond to laser irradiation can be identified. These are, in order of increasing laser power, annealing, buried graphite layer formation, and melting followed by graphitization. The temperature rise during the laser pulse was estimated by solving the three-dimensional heat equation using a modification of the SLIM code [15]. At the spot center, the calculated temperature for annealing ($10 < I < 23$ J/cm^{2}pulse) is $3970 < T < 5200$ K; for buried graphitization ($23 < I < 28$ J/cm^{2}pulse), $5200 < T < 5700$ K; and for melting followed by graphitization ($I > 30$ J/cm^{2}pulse), $T > 5800$ K.

These temperatures, taken with the estimated pressures discussed above, and with the observation that the range

of observed phenomena (i.e, annealing, internal graphitization, and melting) occur over a narrow range of laser powers, and that in particular there is a narrow power window for buried brown spot formation, all point to the interpretation of the data with reference to the portion of the phase diagram close to the triple point.

Annealing occurs when the temperature in the damaged diamond during the laser pulse is in the diamond stable region of the phase diagram (zone A in Fig. 1). Under these P-T conditions, the optical, channeling, and depth profile data confirm that laser irradiation has annealed some of the ion-implantation damage without graphitization or ablation. The suppression of the graphitic phase is a clear indication of the high pressure prevailing in the buried damage layer. Once again we stress that in the absence of a surface cap to generate such pressures laser irradiation has always been found to either graphitize or ablate diamond [6] which is consistent with the phase diagram for low pressures. The remarkable aspect of the annealing in zone A is its rapidity, with regrowth occurring in only tens of nanoseconds.

At slightly higher powers the formation of the brown spots suggests that *internal* graphitization has occurred [Fig. 2(b)]. This occurs with the cap still intact, and hence with the maintenance of high internal pressures, but at a temperature higher than that which gave rise to optimal annealing. This is consistent with moving along a line of constant pressure in Fig. 1 from zone A across the diamond/graphite interface into zone B (graphite stable) in the phase diagram. It should also be noted that both annealing and internal graphitization are observed in a single laser spot, with the latter occurring in the middle of the spot where the laser power is more intense, and therefore the temperature is higher. This is confirmed by the temperature calculations which show that the temperature decreases by about 1000 K at a distance of 2 μm from the spot center.

At even greater power levels graphitization all the way to the surface occurs, as is evidenced by the fact that the entire surface cap and damaged layer can be etched by hot acids. The fact that at this stage a single laser pulse of only 14 ns duration can cause an abrupt transformation of more than 1.5 μm of material indicates that the process, which was initiated deep inside the diamond, has propagated at a speed in excess of 10 m/s. Such high velocities are consistent with the abrupt liquification of the whole of the top layer, i.e., crossing the line in the phase diagram into zone C where carbon is a liquid. With the originally undamaged surface cap now completely transformed, the internal pressure is released and the system is now in the high-temperature, low-pressure regime previously explored by laser-induced melting of graphite [16]. In this regime, the liquid carbon cools and solidifies as graphite.

Finally, we note that the fact that deep implants in diamond can be annealed by short laser pulses, avoiding graphitization, is not only scientifically interesting, but may also have important technological implications with regard to the possibility of doping diamond by the implantation of donor and acceptor ions; a necessary step towards the realization of optoelectronic devices in this wide-band-gap, radiation-hard semiconductor.

The support of the Australian Research Council and the Department of Industry, Technology and Commerce are gratefully acknowledged. R.K. thanks the School of Physics at Melbourne University for warm hospitality. We gratefully acknowledge the assistance of Paul Spizzirri, Sean Dooley, and Rob Elliman.

[1] F. P. Bundy, Physica (Amsterdam) **156A**, 169 (1989), and references therein.

[2] M. van Thiel and F. H. Ree, Int. J. Thermophys. **10**, 227 (1989).

[3] J. F. Ziegler, J. P. Biersack, and U. Littmark, *The Stopping and Range of Ions in Solids* (Pergamon, New York, 1985).

[4] T. E. Derry, J. F. Prins, C. C. P. Madiba, J. Ennis, R. A. Spits, and J. P. F. Sellschop, Nucl. Instrum. Methods Phys. Res., Sect. B **35**, 431 (1988).

[5] G. Braunstein and R. Kalish, Nucl. Instrum. Methods Phys. Res. **209/210**, 387 (1983).

[6] M. Rothchild, C. Arnone, and D. J. Ehrlich, J. Vac. Sci. Technol. B **4**, 310 (1986).

[7] G. S. Sandhu, B. Liu, N. R. Parikh, J. D. Hunn, M. L. Swanson, Th. Wichert, M. Deicher, and H. Skudlik, Mater. Res. Soc. Symp. Proc. **162**, 189 (1990).

[8] M. H. Grimsditch, E. Anastassakis, and M. Cardona, Phys. Rev. B **18**, 901 (1978).

[9] J. Walker, Rep. Prog. Phys. **42**, 1605 (1979).

[10] D. N. Jamieson, R. A. Brown, C. G. Ryan, and J. S. Williams, Nucl. Instrum. Methods Phys. Res., Sect. B **54**, 213 (1991).

[11] S. Prawer, R. Kalish, and M. Adel, Appl. Phys. Lett. **48**, 1585 (1986).

[12] S. Prawer, D. N. Jamieson, S. P. Dooley, P. Spizzirri, K. P. Ghiggino, and R. Kalish, Mater. Res. Soc. Symp. Proc. **235**, 431 (1992).

[13] M. G. Allen, S. Prawer, and D. N. Jamieson (unpublished).

[14] J. F. Prins, T. E. Derry, and J. P. F. Sellschop, Phys. Rev. B **34**, 8870 (1986).

[15] R. Singh and J. Viatella, "Simulation of Laser Interaction with Materials (SLIM)," University of Florida, 1992 (unpublished).

[16] T. Venkatesan, D. C. Jacobson, J. M. Gibson, B. S. Elman, G. Braunstein, M. S. Dresselhaus, and G. Dresselhaus, Phys. Rev. Lett. **53**, 360 (1984).

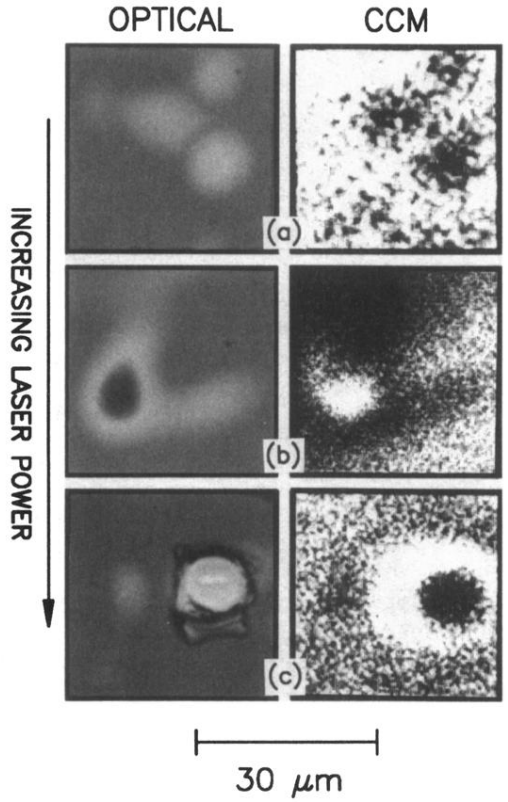

FIG. 2. Transmitted white light optical images and channeling contrast microscopy (CCM) images of laser-irradiated, radiation-damaged (3×10^{15} C^+/cm^2 at 2.8 MeV) diamond. In the optical images, damaged diamond appears dark and annealed or undamaged diamond appears light. In the corresponding CCM images, annealed diamond, which produces a low-intensity backscattered yield, appears dark. Top row (a): Three low-power ($I < 23$ J/cm^{2}pulse) laser spots which have caused partial regrowth. Middle row (b): Intermediate laser powers ($23 < I < 28$ J/cm^{2}pulse) produce a buried brown spot which has a high backscattered yield but is surrounded by a halo of annealed material. Bottom row (c): High laser power ($I > 30$ J/cm^{2}pulse) causes graphitization of the entire surface cap which after chemical etching reveals the underlying high-quality crystal. Swelling of the surrounding material producing a halo of misaligned crystal appears as a bright annulus in the CCM image.